Characterization and properties of antimony doped $Bi_{1.6}Pb_{0.3}Sr_2Ca_3Cu_4O_x$ ceramics

Y. L. CHEN, R. STEVENS
School of Materials, Leeds University, Leeds LS2 9JT, UK

The influence of Sb_2O_3 dopant on the superconductivity and the phase formation of the Bi(Pb)–Sr–Ca–Cu–O system was studied using differential thermal analysis/thermogravimetric analysis (DTA/TGA), X-ray diffraction (XRD), transmission electron microscopy (TEM), a.c. susceptibility and resistance measurements. It was found that the solubility of Sb^{3+} in the 110 K superconducting phase is limited; instead Sb^{3+} readily combines with other elements to form one or more unknown second phase(s), which melt at lower temperatures and accelerates the formation of the 110 K phase. Resistance measurements show the transition initiation temperature of the 110 K superconducting phase is unchanged but that T_c (zero) was found to decrease from 107 K to 98 K. TEM examination generating lattice images from antimony-doped crystals, showed the structure to be inhomogeneous and to contain many defects.

1. Introduction

Recently superconductivity has been observed above 100 K in two classes of oxides, namely, Bi(Pb)–Sr–Ca–Cu–O [1] and Tl–Ba–Ca–Cu–O [2]. Whilst in the case of the thallium compounds, zero resistance has been obtained at 125 K, for the bismuth compounds zero resistance at 107 K has been obtained only by the partial substitution of Pb^{2+} for Bi^{3+} [3]. Without such a substitution, steps are observed in the resistivity plot and zero resistance is obtained around 75–80 K [4]. In a recent study [5], it was reported that the addition of a small amount of Sb^{3+} can substantially raise the superconducting temperature of the bismuth compound, i.e., to 135 K; no account was given of the mechanism of such a substitution. On the other hand, other publications [6, 7] have given conflicting reports on the role of Sb^{3+}; significant solubility of Sb^{3+} in the high-T_c phase was not observed and superconducting phases other than 80 K and 110 K phases were not observed.

There is clearly a need to further examine and explain the effect of Sb^{3+} on the high-T_c phase formation and on the superconducting properties of the bismuth compounds. The present paper describes the synthesis of a bismuth compound with the nominal composition $Bi_{1.6}Pb_{0.3}Sb_{0.1}Sr_2Ca_3Cu_4O_x$; the effect of Sb^{3+} addition was studied using XRD, TEM, a.c. susceptibility and four-probe resistivity measurement. The results were then compared with those of a similar composition without Sb^{3+}, namely, $Bi_{1.6}Pb_{0.4}Sr_2Ca_2Cu_4O_x$. The fabrication and properties of the 110 K phase have been reported in detail elsewhere [3].

2. Experimental details

Appropriate amounts of high purity chemicals, Bi_2O_3, PbO, Sb_2O_3, $SrCO_3$, $CaCO_3$ and CuO were mixed with a small amount of acetone and ground using an agate mortar and pestle. The mixed sample was then used for DTA/TGA studied to determine the reaction temperatures for the formation of the superconducting phases and to check the temperatures at which the carbonates decomposed. The pelletized sample was subsequently fired at 845° C (as predetermined by a DTA/TGA study) for 20, 40, 30 and 50 h with intermediate grinding and repelletizing (Table I).

XRD was carried out using a Philips diffractometer (PW 1710) with CuK_α radiation at a scanning speed of $1°$ min^{-1}. The refinement of the lattice parameters was made using standard computer programs.

Jeol-200CX and Philips EM430 transmission electron microscopes were used to study the microstructure of the dense sample; for the TEM study the sample was prepared by polishing a thin slice to about 30 μm using successively finer grades of diamond paste, followed by ion beam thinning in argon.

Electrical resistivity measurements were performed on a sintered sample strip of approximately 11 mm $\times$ 2 mm $\times$ 1 mm using the standard four-probe technique involving a computer-controlled helium gas flow cryostat; 10 mA current was applied.

The a.c. susceptibility was measured as a function of temperature upon cooling, on powder samples using a mutual inductance technique; a 40 Hz frequency was employed.

TABLE I The list of samples and sintering times

Code	Sb_2O_3 addition	Sintering time (h)
A	Yes	20
B	Yes	20 + 40
C	Yes	20 + 40 + 30
D	Yes	20 + 40 + 30 + 50
F	No	20 + 40 + 80
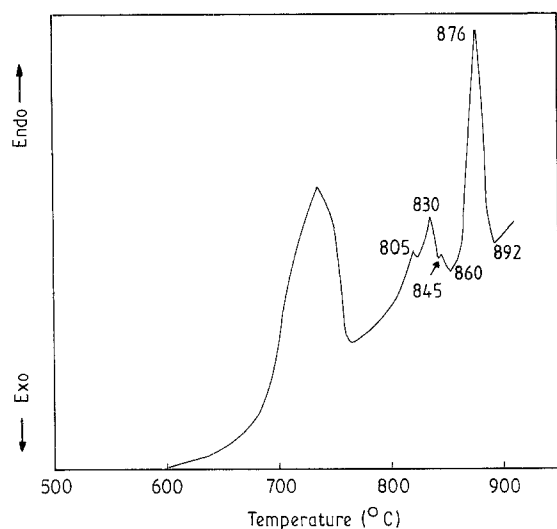
Figure 1 A DTA curve of the powder mixture for $Bi_{1.6}Pb_{0.3}Sb_{0.1}Sr_2Ca_3Cu_4O_x$.

3. Results and discussion

The DTA peak (endothermic on heating) which occurs at a temperature just below the melting peak has been identified as corresponding to the formation of the 110 K phase [3]. The same experiment has been repeated on this composition and the temperature of this peak identified as 845° C (Fig. 1), hence the sample pellets were annealed at 845° C for different times (Table I), in order to obtain densification and growth of the high-T_c phase.

Fig. 2 shows the XRD patterns for antimony-doped sampled B, C, D and the antimony-free sample F. The presence of unidentified XRD peaks shown in samples B, C, D indicate that the formation of second phase(s) in antimony-doped samples is in evidence. The development of other phases would suggest that the solubility of Sb^{3+} in the 110 K phase is limited. This is not
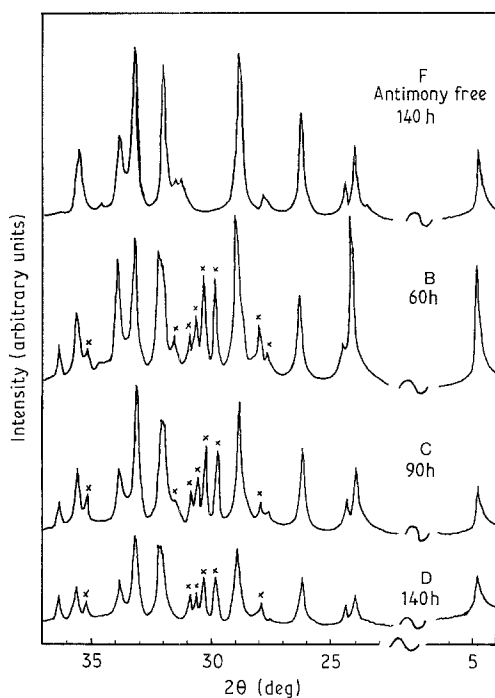

Figure 2 XRD patterns for Sb_2O_3 doped samples, B, C, D and Sb_2O_3 free sample F. The crossed peaks are of the unknown second phase materials.
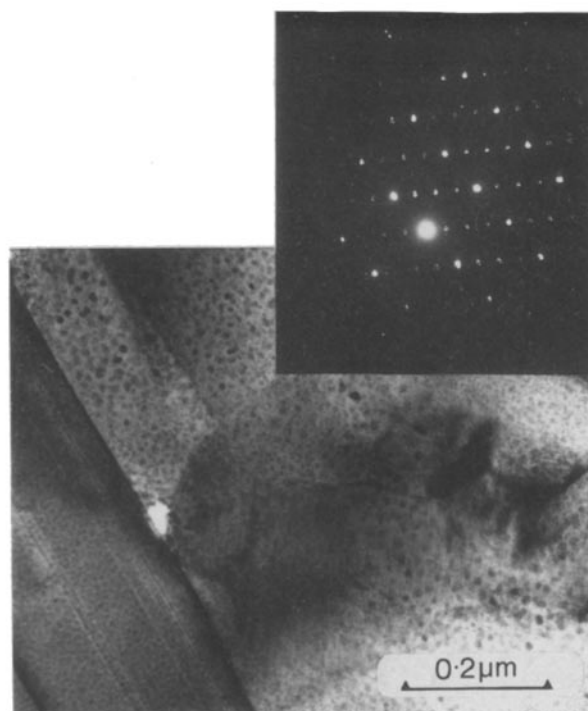

Figure 3 TEM micrograph showing the superconducting phase together with a second phase (unidentified).

unexpected in view of the incompatible size of the respective ions. The ionic radius of Bi^{3+} is 0.096 nm but that of Sb^{3+} is 0.076 nm for 6-fold coordination [8]. Because of the difference in the size of the ions (larger than 20%), it is difficult for Sb^{3+} to directly substitute for Bi^{3+} in the lattice of superconducting phase. However, the reactivity of Sb^{3+} allows it to readily form solid solutions and particularly, amorphous phases with other elements. The polished surface and the fracture surface of the sintered samples have been examined by using SEM/EDAX, but the phases responsible for the unidentified XRD peaks remain to be categorized. However, the existence of the second phase has been confirmed by TEM experiments. Fig. 3 shows a diffraction pattern and a crystal of a second phase, which again cannot be identified as being of the superconducting phases.

Samples with and without the addition of antimony were sintered at the same temperature for different periods of times. From the XRD results (Fig. 4) and a.c. susceptibility measurement (Fig. 5), it is noted that a small XRD peak at $2\theta = 5.8$ deg is present and also, there is a small step at 80 K in the curve of a.c. susceptibility. This is so for the antimony-free sample sintered for 60 h but not for the antimony-doped sample sintered for the same time. It is apparent that the 80 K phase can be eliminated by use of a shorter sintering time (60 h), compared to that needed for the sample without addition of antimony. This strongly infers that the formation of the 110 K phase was enhanced by the addition of antimony. It may well be that Sb_2O_3 facilitates the formation of a liquid phase and this then accelerates the 110 K phase formation. This suggestion is supported by results from a thermal cycling of the powder mixture. Fig. 6 shows a DTA curve of the thermal cycling from 760° C to 890° C of
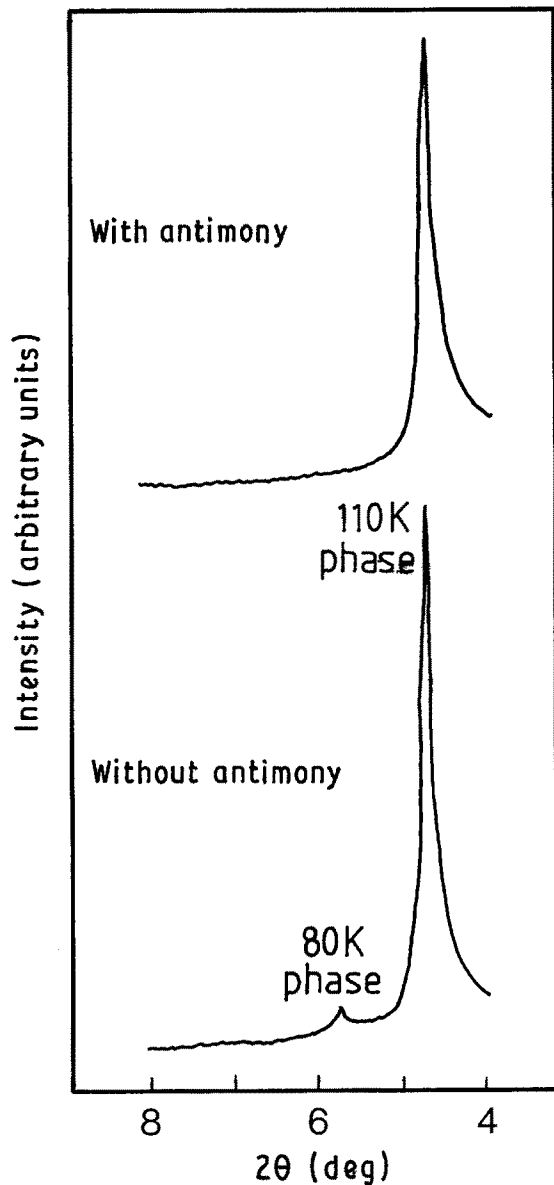
193

Figure 4 A weak XRD peak at $2\theta = 5.8\,\text{deg}$ showing a small amount of 80 K phase remaining in antimony-free samples sintered for 60 h.

tion of 110 K phase. Peak 'b' at 860°C has been identified as due to the melting of the 110 K phase [3]. The exothermal peak (I) has also been identified as being due to the crystallization of the 110 K phase.

There is another exothermal peak (II) at a lower temperature, but this peak is believed to result from the crystallization of the second phase which has a lower melting temperature. Since the second phase(s) melt(s) at a lower temperature than the 110 K phase formation temperature, it will accelerate the diffusion processes and enhance mass transfer, which also helps to densify the sample pellet. The sample pellet of antimony-doped specimen has a higher density ($5.21\,\text{g cm}^{-3}$) than that of antimony-free specimen ($4.94\,\text{g cm}^{-3}$), which again leads support to the proposition that a liquid phase is present at the sintering temperature (liquid phase has also been observed using TEM), thereby increasing the final density of the pellets.

Curves B and C are from the 8th and 14th thermal cycles. It has been noted that peak B, during heating, has been shifted from 860°C to 864°C. Peak II became weak during cooling but another peak (III) appeared, which is adjacent to the position for the crystallization of the 110 K phase. This suggests that another phase(s) might well crystallize from the liquid phase.

The difference in development of the a.c. susceptibility between the antimony-free and antimony-doped samples can be observed in Fig. 5. The lower T_c phase(s) is not only present in the shorter time sintering sample, (20 h), but also reappears in the longer time sintering samples (140 h) for the antimony-doped composition. This phenomena does not occur for antimony-free samples. Samples sintered for 60 h have a maximum amount of the 110 K phase. Although there are not significant differences in the XRD patterns for these specimens, the results for the a.c. susceptibility and thermal analysis indicate that not only could second phases be formed but also that lower T_c phase(s) reoccurs after a longer heat treatment time. This might possibly be due to the effect of long heat treatment times on the samples of 845°C resulting in a lower viscosity of the liquid phase and this also causes changes in the composition of the liquid phase. The lower T_c phase(s) may then be the preferred phase

the powder mixture. Curve A is from the 3rd thermal cycle of the sample. There are two endothermal peaks occurring during the heating. Peak 'a' at 845°C is believed to be due to the combination of the melting of the second phases and the reaction for the forma-
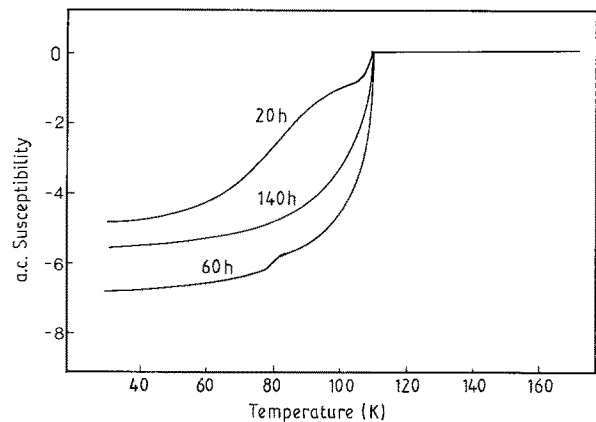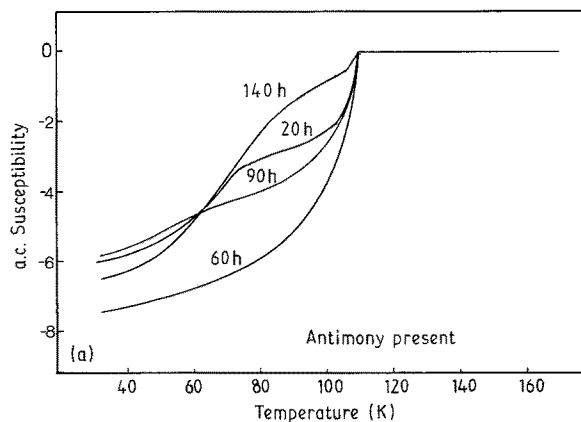

Figure 5 The a.c. susceptibility against temperature for (a) antimony-doped samples; (b) antimony-free samples, sintered for different periods of time.
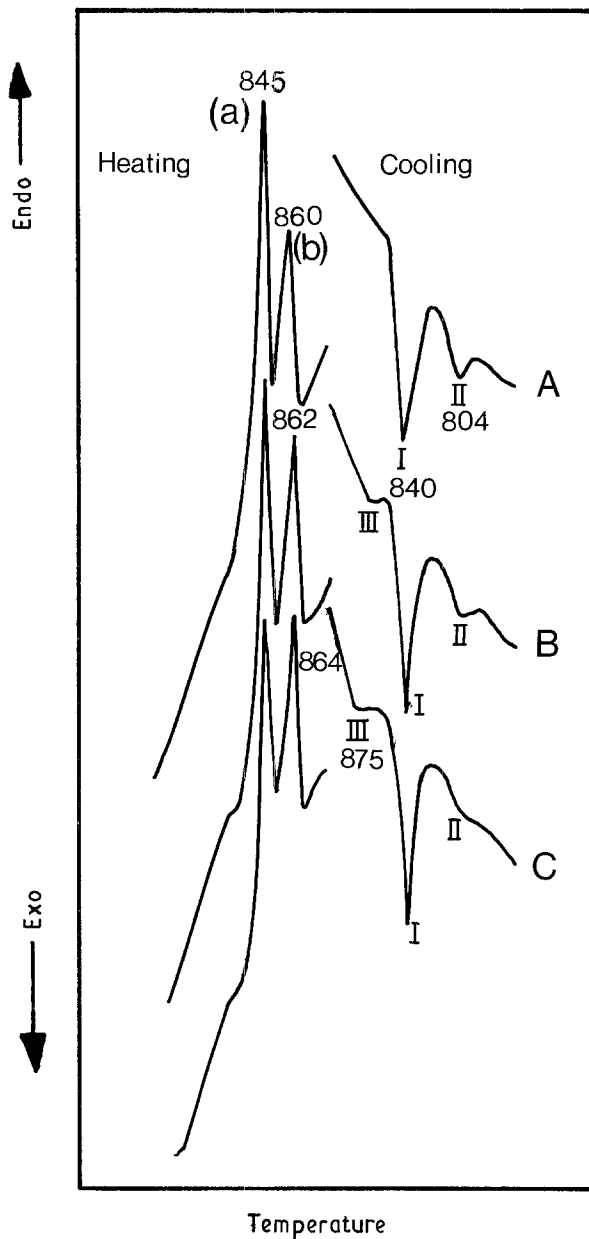
194

Figure 6 DTA curves from the thermal cycling of the powder mixture showing the existance of a second phase with a lower melting temperature (peak II) and a phase with higher melting temperature (peak III) which occurred after the sample had undergone long time thermal cycling.

Figure 7 Temperature dependence of the electrical resistance for the Sb_2O_3 doped superconductor, B, C, D and for the Sb_2O_3-free superconductor, F.

reproducible lattice image, whilst that of the antimony-doped superconducting phase is less regular and contains inhomogeneities. The lattice image exhibits a variation in the size of the unit cell, Fig. 8, where the two, three and four CuO layer units are marked. It is to be noted in the XRD traces that a few peaks coalesce at $2\theta = 32$ deg (Fig. 2); this is possibly due to the presence of second phase XRD peaks very near to the (1 1 9) d peak of 110 K phase. Alternatively a small amount of antimony could diffuse into the lattice

to first crystallize from it. It can be concluded that the presence of Sb_2O_3 in the samples facilitates the formation of a liquid phase and hence accelerates the process of the 110 K phase formation. On the other hand, the presence of such a liquid phase complicates the process chemistry and development of the microstructure, in that the lower T_c phase(s) may be the first to crystallize from the liquid phase.

Fig. 7 shows the variation of resistance with temperature for antimony-doped and antimony-free superconductors. It is clearly apparent that the T_c of the superconducting phase is unchanged but the T_c (zero) has been suppressed to 98 K in antimony-doped sample, a 9 K decrease compared to T_c (zero) of 107 K in the antimony-free sample. The R-T curves undergo little further change even after the samples have been sintered for a further 80 h.

Microstructural examination using TEM shows that the crystals of the undoped 110 K phase give a
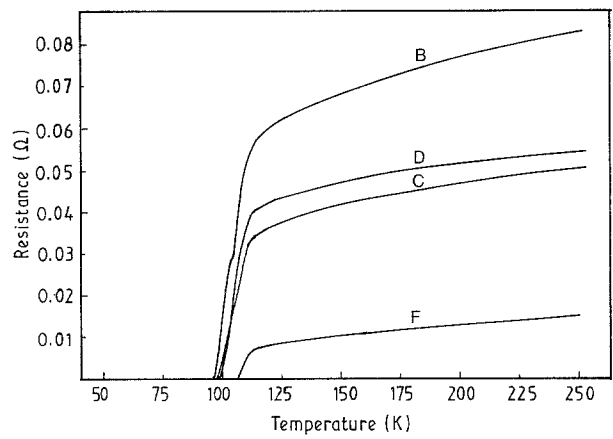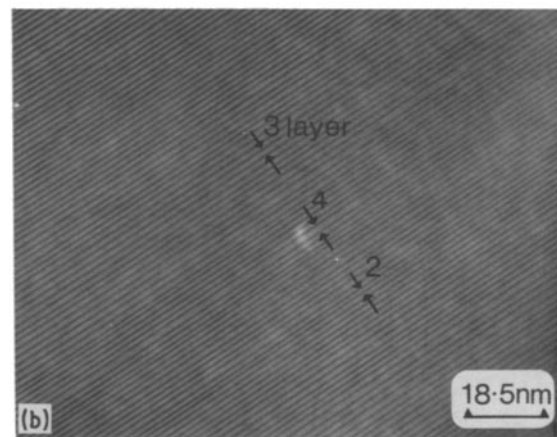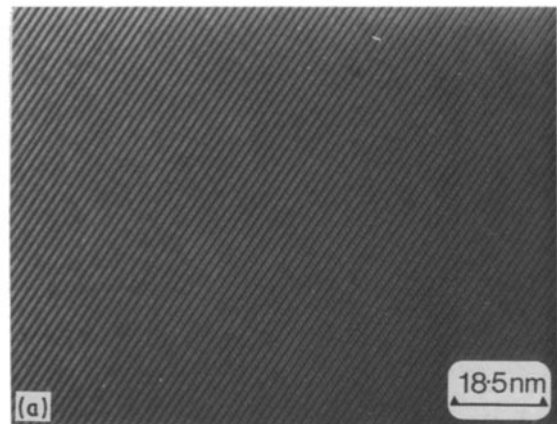

Figure 8 Lattice images of crystals (a) free of Sb_2O_3 addition, (b) with Sb_2O_3 addition. Note the varied spacing of the lattice fringes in (b).
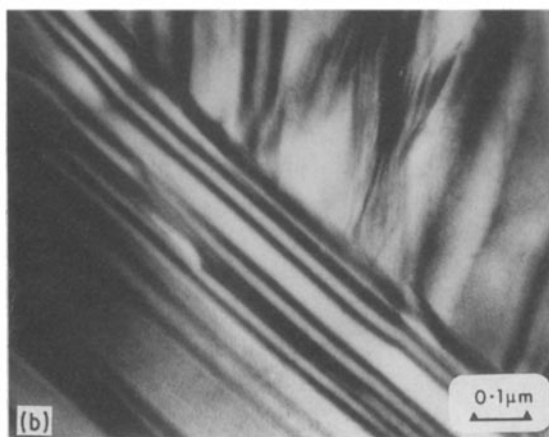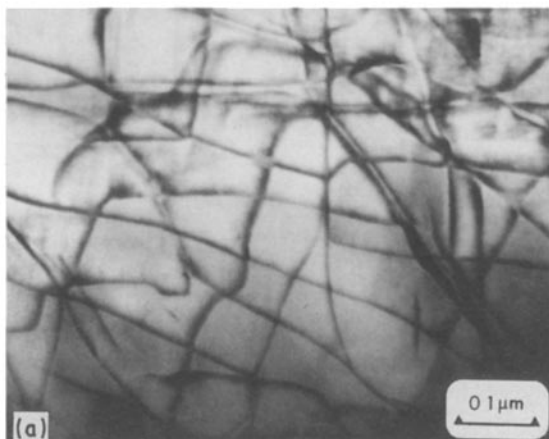
Figure 9 Microstructure of samples containing Sb_2O_3 addition showing (a) dislocation networks, (b) multiple twinning or stacking faults in the superconducting phase.

free sample. This also supports the observation that the solubility of antimony in the superconducting phase is low. The attempted substitution of antimony for bismuth in the lattice of the unit cell leads to complex chemistry with the production of secondary phases of unknown composition.

Defects such as dislocations, networks of dislocations and twinning were observed in antimony-doped samples (Fig. 9). These defects in conjunction with the intercalation of the two, three and four CuO layer units may help account for the reduction in the T_c (zero) of the 110 K superconducting phase.

4. Conclusions

It has been shown that significant amounts of Sb^{3+} could not be dissolved in the 110 K superconducting phase in the bismuth compound. The antimony addition instead formed second phases, which were found to melt at lower temperatures and accelerate the formation of the 110 K phase. Any indication of a phase with a T_c higher than 110 K was not observed. Resistivity studies showed a slight suppression of the T_c (zero) of the superconducting phase, which may be due to a minor amount of antimony dissolved in the lattice. The antimony present in the melt can lead to complex second phase chemistry and to microstructural changes which also might contribute to the change in T_c (zero).

Acknowledgements

and this would then produce a small shift in the d_{119} spacing.

The lattice parameter refinement for antimony and antimony-free samples is given in Table II. It indicates that the unit cell of the 110 K phase containing Sb_2O_3 becomes slightly smaller than that of the antimony-

TABLE II Lattice parameter data for the three samples A, B, C.

Code	Sb_2O_3 addition	Lattice parameters (nm)		
		a	*b*	*c*
B	Yes	0.5385	0.5391	3.698
C	Yes	0.5385	0.5412	3.711
D	Yes	0.5399	0.5410	3.715
F	No	0.5412	0.5412	3.713

References
1. H. MAEDA, Y. TANAKA, M. FUKUTOMI and T. ASANO, *Jpn. Appl. Phys.* **27** (1989) 209.
2. Z. Z. SHENG and A. M. HERMANN, *Nature* **332** (1988) 138.
3. Y. L. CHEN and R. STEVENS, *J. Mater. Sci.*, in press.
4. J. M. TARASCAN, Y. LAPAGE, L. H. GREENE, B. G. BAGLEY, P. BARBOUX, D. M. HUANG and G. W. HULL, *Phys. Rev. Lett.* **38** (1988) 2504.
5. H. B. LIU *et al.*, *Solid State Commun.* **69** (1989) 867.
6. W. PENG, R. H. HANNON, H. LEE, A. P. GENIS, V. J. MELIM and C. W. KIMBALL, *Phys. Lett. A: Cond. Mat. Phys.* **139** (1989) 191.
7. S. X. DOU, H. K. LIU, N. X. TAN, Y. J. SHENG and W. K. JONES, *Physica C* **158** (1989) 97.
8. H. YANAGIDA, "Electronic Materials" (Technological Press, Tokyo, 1975).